

Dynamic nuclear polarization with three electrons in a vertical double quantum dotA. O. Badrutdinov,^{1,*} S. M. Huang,^{2,†} K. Ono,³ K. Kono,³ and D. A. Tayurskii⁴¹*Quantum Dynamics Unit, Okinawa Institute of Science and Technology, Tancha 1919-1, Okinawa 904-0495, Japan*²*Department of Physics, National Sun Yat-Sen University, Kaohsiung, Taiwan 80424, Republic of China*³*Low Temperature Physics Laboratory, RIKEN, Hirosawa 2-1, Wako 351-0198, Japan*⁴*Institute of Physics, Kazan Federal University, Kremlevskaya 18, Kazan 420008, Russia*

(Received 12 March 2013; revised manuscript received 17 June 2013; published 8 July 2013)

We report the observation of dynamic nuclear polarization in a vertical double quantum dot, as a result of a hyperfine interaction with three confined electrons. Our data allow us to distinguish three pumping regimes, characterized by different magnitudes and directions of polarization. Corresponding electron-nuclear spin dynamics is understood by considering relevant three-electron states mixed by hyperfine interaction. Also, an extremely long nuclear spin relaxation time is reported.

DOI: [10.1103/PhysRevB.88.035303](https://doi.org/10.1103/PhysRevB.88.035303)

PACS number(s): 73.63.Kv, 73.23.Hk, 76.60.Es

I. INTRODUCTION

The effect of dynamic nuclear polarization (DNP) in GaAs-based quantum dot nanostructures¹⁻⁴ has been recognized as an issue of great importance in the context of spin-based quantum computation. While fluctuations of the nuclear hyperfine field acting on confined electrons cause fast decoherence of electron spin states,⁵⁻⁷ DNP allows us to improve the coherence time by narrowing the distribution of hyperfine field fluctuations.⁸⁻¹¹ Compared to alternative ways to overcome decoherence, such as using spin-echo pulse sequences,^{7,12,13} or by defining the quantum dot in silicon instead of GaAs,^{14,15} DNP is relatively easy to implement. Furthermore, it allows universal quantum control over two-electron spin qubits.¹⁶ Ensembles of polarized nuclear spins, as well as hybrid electron-nuclear spin systems, were also considered as potential quantum computational tools.¹⁷⁻²³ Direct electrical control over the nuclear spin bath was implemented in a vertical double quantum dot system,²² demonstrating that the coherence time of the nuclear spin ensemble is on the order of milliseconds.

In quantum dots DNP is achieved by either the optical pumping technique,^{9,24-31} or by making use of the Pauli spin blockade phenomenon.³²⁻³⁵ When the latter was initially employed in double quantum dot systems, it was based on hyperfine-induced relaxation of a two-electron $S = 1$ triplet spin state.³³ Recently, more complicated triple quantum dot systems, which are expected to provide additional tools for future quantum information processing applications,^{36,37} and which allow the creation and manipulation of higher-spin electron states, have attracted much attention.³⁸⁻⁴⁵ Thus, it would be of interest to explore the possibility of creating DNP with high-spin states involving more than two electrons. In fact, a spin blockade regime, involving three-electron $S = 3/2$ quadruplet spin states, has already been reported in triple⁴⁵ and double⁴⁶ quantum dot systems. However, to the best of our knowledge, DNP associated with the quadruplet spin blockade still needs to be reported.

In this paper we report an investigation of DNP mechanisms in a vertical double quantum dot in the quadruplet spin blockade (Q-SB) regime. Our data demonstrate the emergence of DNP and suggest that there exist three distinct regimes of nuclear pumping. We consider the energy diagram of relevant three-electron spin states, which could be mixed

by a hyperfine interaction, and show that observed pumping regimes can be consistently explained in terms of hyperfine-induced spin blockade lifting. We also study nuclear spin relaxation dynamics and reveal that the lifetime of DNP can be extremely long.

II. EXPERIMENT

Figure 1(a) shows a schematic view of the vertical double quantum dot device, which is a roughly 0.4- μm -diam pillar etched from a GaAs-based heterostructure. Quantum dots are formed in two 12-nm-thick $\text{In}_{0.06}\text{Ga}_{0.94}\text{As}$ potential wells, interspersed between three $\text{Al}_{0.22}\text{Ga}_{0.78}\text{As}$ layers, forming outer (7.5 nm) and central (6.5 nm) potential barriers. The whole structure is surrounded by a Ti/Au gate electrode. We measured current through the dot (I_{dot}) versus source-drain voltage (V_{SD}) and gate voltage (V_{G}). All measurements, if not specified otherwise, were performed on a dilution refrigerator with a base temperature of 10 mK. The corresponding effective electron temperature was estimated to be about 0.2 K from the resonance tunneling peak width at low bias.⁴⁷

III. RESULTS AND DISCUSSION

Differential conductance $dI_{\text{dot}}/dV_{\text{SD}}$ plotted versus V_{SD} and V_{G} is shown in Figs. 1(b) and 1(c). Both data sets are obtained by measuring I_{dot} while V_{SD} is swept repeatedly at different values of V_{G} ; however, Fig. 1(b) corresponds to a V_{SD} sweep from negative to positive values, while in Fig. 1(c) the sweep direction is the opposite. In the white diamond-shaped regions of the plot, $I_{\text{dot}} \approx 0$ due to the Coulomb blockade effect.^{48,49} Suppression of I_{dot} at positive V_{SD} outside the $N = 3$ Coulomb blockade region (N is the number of confined electrons) is caused by the formation of a three-electron $S = 3/2$ quadruplet state, sketched in Fig. 1(d). Here one electron resides in dot 1 and two other electrons occupy different orbital states⁴⁸ in dot 2. Since all electrons have the same direction of spin, tunneling of an electron from dot 1 to either of the half-occupied orbital states of dot 2 is prohibited by the Pauli exclusion principle (for details see the recent work by Amaha *et al.*⁴⁶). In fact, the electrochemical potentials of electron states, involved in the formation of Q-SB, strongly depend on the external magnetic field B applied perpendicular to the dot heterostructure

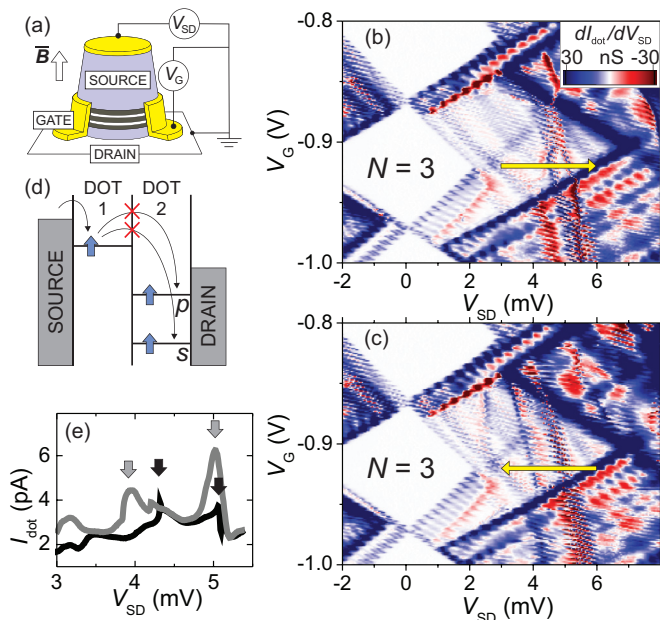


FIG. 1. (Color online) (a) Schematic view of the GaAs vertical double quantum dot device. (b), (c) $dI_{\text{dot}}/dV_{\text{SD}}$ vs V_{SD} and V_G . (b) is obtained by sweeping V_{SD} from -2 to 8 mV at different V_G , while (c) is obtained by sweeping V_{SD} from 8 to -2 mV. N indicates the number of confined electrons in a particular Coulomb blockade region. (d) Electrochemical potential diagram illustrating the mechanism of Q-SB emergence. (e) I_{dot} vs V_{SD} , measured by sweeping V_{SD} up (black trace) and down (gray trace), at $V_G = -0.92$ V [along the arrows marked on (b) and (c)].

plane.⁴⁸ In order to have a Q-SB regime in our quantum dot, all measurements were done at $B = 3$ T. The gridlike pattern of Coulomb blockade regions observed in Figs. 1(b) and 1(c) results from the quantized energy spectrum of the electron source [Fig. 1(a)], which becomes resolved at low enough temperature. That phenomenon is described in a separate paper⁵⁰ and does not influence the following discussion.

As one can see from a comparison of Figs. 1(b) and 1(c), within the Q-SB regime, the hysteretic behavior of I_{dot} with respect to the V_{SD} sweep direction is observed. Figure 1(e) shows the traces of I_{dot} vs V_{SD} along the arrows marked in Figs. 1(b) and 1(c) ($V_G = -0.92$ V). The positions of certain I_{dot} maxima clearly depend on the sweep direction. Such behavior is known to be a manifestation of DNP formation in a conventional spin blockade regime.^{32,33} There, the characteristic changes of I_{dot} indicate conditions in which a certain two-electron $S = 1$ triplet state is mixed with an $S = 0$ singlet state by a hyperfine interaction, allowing spin blockade lifting accompanied by a nuclear spin flip.^{22,33} Repeated nuclear spin flips result in the accumulated nuclear polarization, which alters the conditions of S - T mixing by means of an effective magnetic field, causing hysteresis. Thus, our data suggest that in the Q-SB regime nuclear pumping is also occurring.

A. DNP pumping

To further explore DNP formation in the Q-SB regime, we performed a pump-probe measurement sequence (in this and

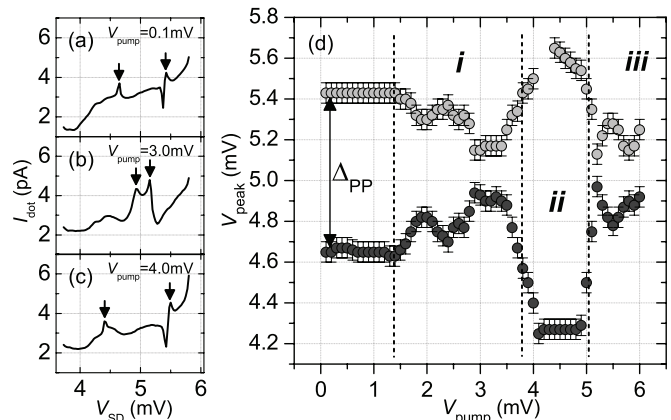


FIG. 2. (a)–(c) I_{dot} vs V_{SD} , measured after pumping the nuclei at different values of V_{pump} . (d) V_{peak} vs V_{pump} : Dark gray symbols correspond to the I_{dot} maximum at lower V_{SD} , and light gray symbols correspond to the I_{dot} maximum at higher V_{SD} . *i*, *ii*, and *iii* indicate V_{pump} ranges within the Q-SB regime, characterized by different signs of I_{dot} maxima displacement with respect to position, corresponding to the $V_{\text{pump}} = 0$ trace. Δ_{PP} denotes the gap between current maxima. Dotted lines are guides for the eye.

the following measurements V_G was set to -0.92 V). Initially, V_{SD} was set to a certain value (V_{pump}) for 10 min, and then the trace of I_{dot} vs V_{SD} was recorded (spanning the range of V_{SD} in which the hysteretic behavior of I_{dot} was observed). V_{pump} was varied in the range 0–6 mV, capturing both Coulomb blockade and Q-SB regimes. The resulting traces are shown in Figs. 2(a)–2(c) for several values of V_{pump} . The values of V_{SD} corresponding to I_{dot} maxima, denoted as V_{peak} , are plotted in Fig. 2(d) as a function of V_{pump} . As expected, for V_{pump} varying within the Coulomb blockade regime, no evolution of the I_{dot} vs V_{SD} trace was observed, since DNP cannot build up under the Coulomb blockade.³³ However, as soon as V_{pump} corresponds to a Q-SB regime, I_{dot} maxima shift with respect to those of a nonpumped trace, indicating DNP emergence. Furthermore, the dependence of the I_{dot} vs V_{SD} trace on V_{pump} within the Q-SB range allows us to distinguish several regimes of pumping (*i*, *ii*, *iii*), characterized by different signs of I_{dot} maxima displacement. The data suggest that DNP pumping is observed throughout the whole range of V_{pump} corresponding to Q-SB.

The observed phenomena can be explained by considering an energy diagram of electron states involved in the formation of Q-SB⁴⁶ [Fig. 3(a)]. Here (N_1, N_2) refers to a charge state with N_1 electrons in dot 1 and N_2 electrons in dot 2; $D(1,2)$, $D_e(1,2)$, and $D(0,3)$ denote (1,2)-ground, (1,2)-excited, and (0,3)-excited states with $S = 1/2$, which are twofold degenerate in zero magnetic field, and $Q(1,2)$ denotes a (1,2)-excited state with $S = 3/2$, which is fourfold degenerate, and which causes Q-SB. The energy of the (0,3) state decreases relative to the energy of (1,2) states with increasing V_{SD} , and due to interdot tunnel coupling, the $D_e(1,2)$ and $D(0,3)$ states are mixed, which leads to their anticrossing.⁴⁶ The presence of an external magnetic field lifts up spin degeneracy, leading to fourfold splitting of the Q state and twofold splitting of D states of the system [Fig. 3(b)]. Nuclear pumping is possible when the Q state is mixed with

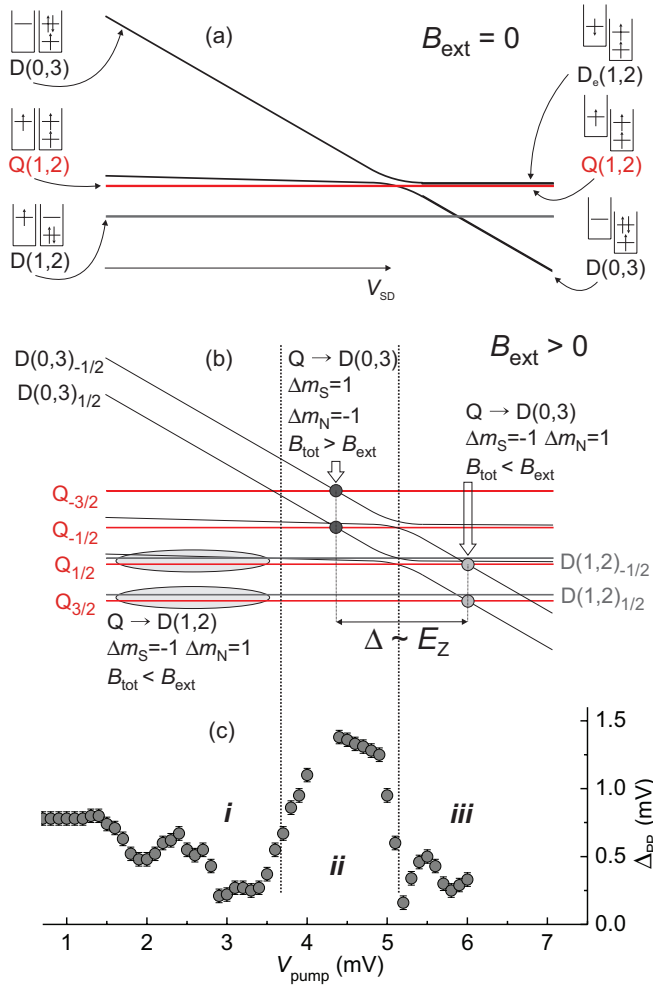


FIG. 3. (Color online) Energy diagrams of three-electron states involved in the DNP pumping, plotted vs V_{SD} , in (a) the absence and (b) presence of an external magnetic field. $D(1,2)$, $D_e(1,2)$, and $D(0,3)$ denote $(1,2)$ -ground, $(1,2)$ -excited, and $(0,3)$ charge states with $S = 1/2$, and $Q(1,2)$ denotes a $(1,2)$ charge state with $S = 3/2$. The gray circles in (b) indicate where Q and D states are mixed by the hyperfine interaction and DNP pumping is possible. The dark gray and light gray circles correspond to the direction of the emerging nuclear field B_N with and against the external field, respectively. (c) Δ_{PP} vs V_{pump} . The dashed-dotted lines are guides for the eye.

one of the D states via a hyperfine interaction. That is the case when the magnetic quantum numbers (m_s) of those states differ by 1, so that mutual electron-nuclear flip-flop processes can happen.^{33,49} As shown in Fig. 3(b), that sort of mixing occurs between Q and $D(0,3)$ states on both sides of the $D_e(1,2) - D(0,3)$ anticrossing. $Q_{-3/2} - D(0,3)_{-1/2}$ and $Q_{-1/2} - D(0,3)_{1/2}$ crossings at lower V_{SD} have $\Delta m_s = 1$ and $\Delta m_n = -1$, while in contrast, $Q_{3/2} - D(0,3)_{1/2}$ and $Q_{1/2} - D(0,3)_{-1/2}$ crossings at higher V_{SD} have $\Delta m_s = -1$ and $\Delta m_n = 1$. The sign of Δm_n determines the direction of nuclear polarization relative to the external magnetic field, giving rise to two pumping regimes, *ii* and *iii*. In GaAs, the effective nuclear field acting on electrons is directed against the nuclear polarization,⁵¹ thus in regime *ii*, the nuclear field (B_N) pumps with the external magnetic field, whereas in regime *iii*, B_N pumps against the external magnetic field.

Furthermore, those $Q - D$ crossings result in leakage current and the observed I_{dot} maxima. Other $Q - D$ crossings, such as $Q_{\pm 3/2} - D(0,3)_{\mp 1/2}$ or $Q_{\pm 1/2} - D_e(1,2)_{\pm 1/2}$, do not result in hyperfine-induced mixing, since they do not satisfy the $m_s = \pm 1$ selection rule, and thus, do not contribute to DNP pumping.

Additional mixing may happen between the Q and $D(1,2)$ states, namely, the $Q_{3/2} - D(1,2)_{1/2}$ and $Q_{1/2} - D(1,2)_{-1/2}$ states [Fig. 3(b)]. The energy gap between those states does not depend on V_{SD} , but depends only on the total magnetic field, which is the sum of the external field B and the nuclear field B_N . If, for a given value of B , those states are close to degeneracy, they can be mixed by hyperfine interaction and cause DNP.³³ In this case $\Delta m_s = -1$ and $\Delta m_n = 1$, so that the nuclear field is directed against the external magnetic field. This pumping mechanism is likely to be responsible for the existence of pumping regime *i*, and probably contributes to pumping regime *iii* as well. In Fig. 3(c) the data shown on Fig. 2(d) are replotted as the gap between I_{dot} maxima, denoted as Δ_{PP} , versus V_{pump} . Comparing Fig. 3(c) with Fig. 3(b) illustrates the correlation between experimentally observed pumping regimes and electron state diagrams, summarizing the above discussion.

From Fig. 3(b) one can see that if Zeeman splitting of electron spin states exceeds interdot tunnel coupling, then it would be related to the gap between two $Q - D(0,3)$ hyperfine-mixed crossings, denoted Δ , as $E_Z = (\alpha \Delta / 2)$, where $\alpha = d[D(0,3) - Q]/dV_{SD}$ reflects the dependence of the energy difference between the $(0,3)$ and $(1,2)$ charge states on V_{SD} , and is proportional to the fraction of V_{SD} that drops between dot 1 and dot 2. The latter can be estimated from the analysis of slopes of specific Coulomb diamond edges;^{49,52} for our device α is about 0.13 eV/V. If we neglect the DNP buildup during the probe sweep, then the measured Δ_{PP} would be exactly equal to Δ , corresponding to B_N established before the probe sweep. Under this assumption, for a certain value of V_{pump} we can estimate the nuclear field as $B_N = B(\Delta_{PP}/\Delta_{PP}^0 - 1)$, where $B = 3$ T is the external field and $\Delta_{PP}^0 \approx 0.8$ mV is the gap between I_{dot} maxima for traces taken after V_{pump} within the Coulomb blockade regime. This estimation gives $-2.3 \leq B_N \leq 2.3$ T in the range of V_{pump} within the Q-SB regime. We can also estimate the g factor of our device as $|g| = E_Z/\mu_B B = (\alpha \Delta_{PP}^0 / 2) / \mu_B B$, or about 0.3. This is in good agreement with values measured previously on similar devices (0.3 and 0.36).^{53,54} However, since the probe sweep time (≈ 30 s) is actually not much less than the characteristic nuclear pumping time (about several minutes), a certain fraction of DNP may build up during the probe sweep. Thus, Δ_{PP} does not exactly reflect Δ , so the above estimations may be not very precise.

B. DNP relaxation

We also observed DNP relaxation dynamics by means of a pump-wait-probe measurement sequence. After pumping DNP at $V_{pump} = 4.7$ mV, V_{SD} was set to a certain value V_{wait} outside the Q-SB regime for a time interval τ , during which DNP relaxed, and then the probe sweep followed. The results are plotted in Fig. 4 as the dependence of Δ_{PP} , normalized to unity, on τ . We first probed relaxation under

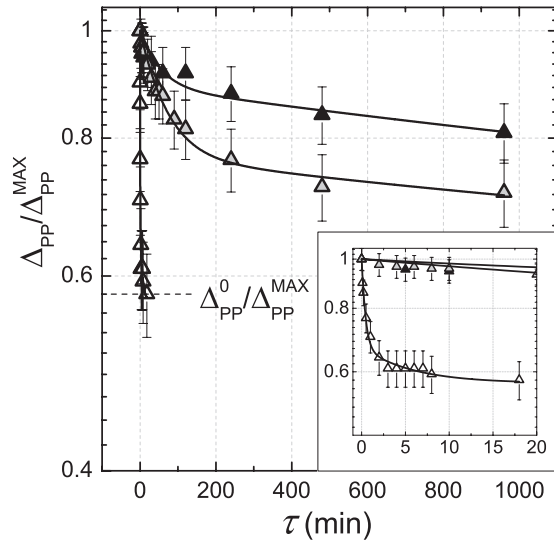


FIG. 4. DNP relaxation data, plotted as $\Delta_{PP}/\Delta_{PP}^{MAX}$ vs τ , under different relaxation conditions: $V_{wait} = 0$ at 0.2 K (black triangles); $V_{wait} = 0$ at 0.9 K (gray triangles); $V_{wait} = -5$ mV at 0.2 K (white triangles). The indicated value $\Delta_{PP}^0/\Delta_{PP}^{MAX}$ corresponds to zero DNP. Solid lines fit experimental data with biexponential decay. The decay rates (in min) are 53 ± 15 and 3348 ± 818 , 68 ± 5 and 2688 ± 570 , and 0.4 ± 0.03 and 5.5 ± 0.8 , correspondingly. The inset shows the same data plotted on a different time scale.

Coulomb blockade conditions, with $V_{wait} = 0$, and found that DNP exists even after 16 h. Increasing temperature seemed to increase the DNP relaxation rate. For reference we tried another condition of relaxation by setting $V_{wait} = -5$ mV, with a negative current of 100 pA flowing through the dot. In this case, relaxation was much faster and did not show any temperature dependence. The best fit of relaxation data was obtained with biexponential decay curves, in agreement with previous studies.⁵⁵ This gives a fast rate of about 1 h and a slow rate of about 50 h for relaxation under a Coulomb blockade regime, although we note significant uncertainty due to experimental error, as indicated in the Fig. 4 legend.

The observed long relaxation of DNP is likely to be explained by the temperature dependence of the nuclear relaxation rate. Previous studies of DNP in vertical quantum

dots, which reported decay time on the order of 10 s, were done at about 1.5 K,^{55,56} in contrast to our measurements below 1 K. On the other hand, similar extremely long-term nuclear spin dynamics has been reported in self-assembled quantum dots pumped by optical resonance at ultralow temperatures.^{30,31} Relaxation at $V_{wait} = -5$ V is also consistent with the temperature dependence scenario, if we take into account that because of Joule heating the actual temperature of the dot could be higher than that measured by a thermometer. Finally, the nuclear relaxation rate in bulk GaAs is known to have a strong temperature dependence.^{57,58} For a better understanding of DNP relaxation mechanisms, a more detailed study will be necessary.

Our result is a demonstration of extremely long-lived DNP in vertical quantum dots. The observed nuclear relaxation time is similar to that reported in self-assembled quantum dots (about 30 h).³¹ That is about three orders of magnitude longer than the nuclear relaxation time measured in laterally defined quantum dots,⁵⁹ which falls in the range of 8–56 s, depending on the external magnetic field and the quantum dot charge state. Together with the presumed scalability of vertical quantum dot devices, long nuclear relaxation time looks favorable for the prospects of using vertical dots in quantum information processing applications, even though much remains to be done.

IV. CONCLUSION

We have demonstrated and explored the emergence of DNP in the three-electron Q-SB regime of a vertical double quantum dot system. The results are well understood in terms of hyperfine-induced spin blockade lifting, considering the relevant three-electron spin states. We also showed that extremely long nuclear spin relaxation times are possible in vertical double quantum dots.

ACKNOWLEDGMENT

We thank S. Aird for his help with editing the manuscript. A.O.B. is supported by an internal grant from Okinawa Institute of Science and Technology (OIST) Graduate University. S.M.H. thanks the financial support from National Science Council through Grants No. NSC 101-2112-M-110-001-MY3.

*alexbadr@oist.jp

†smhuang.py90g@nctu.edu.tw

¹W. A. Coish and J. Baugh, *Phys. Status Solidi B* **246**, 2203 (2009).

²B. Urbaszek, X. Marie, T. Amand, O. Krebs, P. Voisin, P. Maletinsky, A. Hoge, and A. Imamoglu, *Rev. Mod. Phys.* **85**, 79 (2013).

³E. A. Chekhovich, M. N. Makhonin, A. I. Tartakovskii, A. Yacoby, H. Bluhm, K. C. Nowack, and L. M. K. Vandersypen, *Nat. Mater.* **12**, 494 (2013).

⁴R. J. Warburton, *Nat. Mater.* **12**, 483 (2013).

⁵F. H. L. Koppens, J. A. Folk, J. M. Elzerman, R. Hanson, L. H. W. van Beveren, I. T. Vink, H. P. Tranitz, W. Wegscheider, L. P.

Kouwenhoven, and L. M. K. Vandersypen, *Science* **309**, 1346 (2005).

⁶F. H. L. Koppens, C. Buizert, K. J. Tielrooij, I. T. Vink, K. C. Nowack, T. Meunier, L. P. Kouwenhoven, and L. M. K. Vandersypen, *Nature (London)* **442**, 766 (2006).

⁷J. R. Petta, A. C. Johnson, J. M. Taylor, E. A. Laird, A. Yacoby, M. D. Lukin, C. M. Marcus, M. P. Hanson, and A. C. Gossard, *Science* **309**, 2180 (2005).

⁸H. Bluhm, S. Foletti, D. Mahalu, V. Umansky, and A. Yacoby, *Phys. Rev. Lett.* **105**, 216803 (2010).

⁹X. Xu, W. Yao, B. Sun, D. G. Steel, A. S. Bracker, D. Gammon, and L. J. Sham, *Nature (London)* **459**, 1105 (2009).

- ¹⁰D. J. Reilly, J. M. Taylor, J. R. Petta, C. M. Marcus, M. P. Hanson, and A. C. Gossard, *Science* **321**, 817 (2008).
- ¹¹C. Barthel, J. Medford, H. Bluhm, A. Yacoby, C. M. Marcus, M. P. Hanson, and A. C. Gossard, *Phys. Rev. B* **85**, 035306 (2012).
- ¹²F. H. L. Koppens, K. C. Nowack, and L. M. K. Vandersypen, *Phys. Rev. Lett.* **100**, 236802 (2008).
- ¹³H. Bluhm, S. Foletti, I. Neder, M. Rudner, D. Mahalu, V. Umansky, and A. Yacoby, *Nat. Phys.* **7**, 109 (2011).
- ¹⁴B. M. Maune, M. G. Borselli, B. Huang, T. D. Ladd, P. W. Deelman, K. S. Holabird, A. A. Kiselev, I. Alvarado-Rodriguez, R. S. Ross, A. E. Schmitz, M. Sokolich, C. A. Watson, M. F. Gyure, and A. T. Hunter, *Nature (London)* **481**, 344 (2012).
- ¹⁵A. Wild, J. Kierig, J. Sailer, J. W. Ager, and E. E. Haller, *Appl. Phys. Lett.* **100**, 143110 (2012).
- ¹⁶S. Foletti, H. Bluhm, D. Mahalu, V. Umansky, and A. Yacoby, *Nat. Phys.* **5**, 903 (2009).
- ¹⁷L. M. K. Vandersypen and I. L. Chuang, *Rev. Mod. Phys.* **76**, 1037 (2005).
- ¹⁸J. H. Smet, R. A. Deutschmann, F. Ertl, W. Wegscheider, G. Abstreiter, and K. von Klitzing, *Nature (London)* **415**, 281 (2002).
- ¹⁹G. Yusa, K. Muraki, K. Takashina, K. Hashimoto, and Y. Hirayama, *Nature (London)* **434**, 1001 (2005).
- ²⁰G. W. Morley, M. Warner, A. M. Stoneham, P. T. Greenland, J. van Tol, C. W. M. Kay, and G. Aeppli, *Nat. Mater.* **9**, 725 (2010).
- ²¹S. Simmons, R. M. Brown, H. Riemann, N. V. Abrosimov, P. Becker, H. J. Pohl, M. L. W. Thewalt, K. M. Itoh, and J. J. L. Morton, *Nature (London)* **470**, 69 (2011).
- ²²R. Takahashi, K. Kono, S. Tarucha, and K. Ono, *Phys. Rev. Lett.* **107**, 026602 (2011).
- ²³G. W. Morley, P. Lueders, M. H. Mohammady, S. J. Balian, G. Aeppli, C. W. M. Kay, W. M. Witzel, G. Jeschke, and T. S. Monteiro, *Nat. Mater.* **12**, 103 (2013).
- ²⁴S. W. Brown, T. A. Kennedy, D. Gammon, and E. S. Snow, *Phys. Rev. B* **54**, R17339 (1996).
- ²⁵D. Gammon, A. L. Efros, T. A. Kennedy, M. Rosen, D. S. Katzer, D. Park, S. W. Brown, V. L. Korenev, and I. A. Merkulov, *Phys. Rev. Lett.* **86**, 5176 (2001).
- ²⁶A. S. Bracker, E. A. Stinoff, D. Gammon, M. E. Ware, J. G. Tischler, A. Shabaev, A. L. Efros, D. Park, D. Gershoni, V. L. Korenev, and I. A. Merkulov, *Phys. Rev. Lett.* **94**, 047402 (2005).
- ²⁷C. W. Lai, P. Maletinsky, A. Badolato, and A. Imamoglu, *Phys. Rev. Lett.* **96**, 167403 (2006).
- ²⁸P.-F. Braun, B. Urbaszek, T. Amand, X. Marie, O. Krebs, B. Eble, A. Lemaitre, and P. Voisin, *Phys. Rev. B* **74**, 245306 (2006).
- ²⁹C. Latta, A. Hoge, Y. Zhao, A. N. Vamivakas, P. Maletinsky, M. Kroner, J. Dreiser, I. Carusotto, A. Badolato, D. Schuh, W. Wegscheider, M. Atatüre, and A. Imamoglu, *Nat. Phys.* **5**, 758 (2009).
- ³⁰P. Maletinsky, M. Kroner, and A. Imamoglu, *Nat. Phys.* **5**, 407 (2009).
- ³¹C. Latta, A. Srivastava, and A. Imamoglu, *Phys. Rev. Lett.* **107**, 167401 (2011).
- ³²K. Ono and S. Tarucha, *Phys. Rev. Lett.* **92**, 256803 (2004).
- ³³J. Baugh, Y. Kitamura, K. Ono, and S. Tarucha, *Phys. Rev. Lett.* **99**, 096804 (2007).
- ³⁴J. R. Petta, J. M. Taylor, A. C. Johnson, A. Yacoby, M. D. Lukin, C. M. Marcus, M. P. Hanson, and A. C. Gossard, *Phys. Rev. Lett.* **100**, 067601 (2008).
- ³⁵I. T. Vink, K. C. Nowack, F. H. L. Koppens, J. Danon, Y. V. Nazarov, and L. M. K. Vandersypen, *Nat. Phys.* **5**, 764 (2009).
- ³⁶D. P. DiVincenzo, D. Bacon, J. Kempe, G. Burkard, and K. B. Whaley, *Nature (London)* **408**, 339 (2000).
- ³⁷A. D. Greentree, J. H. Cole, A. R. Hamilton, and L. C. L. Hollenberg, *Phys. Rev. B* **70**, 235317 (2004).
- ³⁸M. Korkusinski, I. P. Gimenez, P. Hawrylak, L. Gaudreau, S. A. Studenikin, and A. S. Sachrajda, *Phys. Rev. B* **75**, 115301 (2007).
- ³⁹D. Schroer, A. D. Greentree, L. Gaudreau, K. Eberl, L. C. L. Hollenberg, J. P. Kotthaus, and S. Ludwig, *Phys. Rev. B* **76**, 075306 (2007).
- ⁴⁰E. A. Laird, J. M. Taylor, D. P. DiVincenzo, C. M. Marcus, M. P. Hanson, and A. C. Gossard, *Phys. Rev. B* **82**, 075403 (2010).
- ⁴¹G. Granger, L. Gaudreau, A. Kam, M. Pioro-Ladriere, S. A. Studenikin, Z. R. Wasilewski, P. Zawadzki, and A. S. Sachrajda, *Phys. Rev. B* **82**, 075304 (2010).
- ⁴²C.-Y. Hsieh, Y.-P. Shim, and P. Hawrylak, *Phys. Rev. B* **85**, 085309 (2012).
- ⁴³L. Gaudreau, G. Granger, A. Kam, G. C. Aers, S. A. Studenikin, P. Zawadzki, M. Pioro-Ladriere, Z. R. Wasilewski, and A. S. Sachrajda, *Nat. Phys.* **8**, 54 (2012).
- ⁴⁴S. Amaha, T. Hatano, H. Tamura, S. Teraoka, T. Kubo, Y. Tokura, D. G. Austing, and S. Tarucha, *Phys. Rev. B* **85**, 081301(R) (2012).
- ⁴⁵S. Amaha, W. Izumida, T. Hatano, S. Teraoka, S. Tarucha, J. A. Gupta, and D. G. Austing, *Phys. Rev. Lett.* **110**, 016803 (2013).
- ⁴⁶S. Amaha, W. Izumida, T. Hatano, K. Kono, S. Tarucha, and K. Ono (unpublished).
- ⁴⁷C. W. J. Beenakker, *Phys. Rev. B* **44**, 1646 (1991).
- ⁴⁸L. P. Kouwenhoven, D. G. Austing, and S. Tarucha, *Rep. Prog. Phys.* **64**, 701 (2001).
- ⁴⁹R. Hanson, L. P. Kouwenhoven, J. R. Petta, S. Tarucha, and L. M. K. Vandersypen, *Rev. Mod. Phys.* **79**, 1217 (2007).
- ⁵⁰S. M. Huang, A. O. Badrutdinov, K. Kono, and K. Ono [J. Phys.: Cond. Matt. (to be published)].
- ⁵¹D. Paget, G. Lampel, B. Sapoval, and V. I. Safarov, *Phys. Rev. B* **15**, 5780 (1977).
- ⁵²S. M. Huang, Y. Tokura, H. Akimoto, K. Kono, J. J. Lin, S. Tarucha, and K. Ono, *Phys. Rev. Lett.* **104**, 136801 (2010).
- ⁵³S. M. Huang, H. Akimoto, K. Kono, J. J. Lin, S. Tarucha, and K. Ono, *Jpn. J. Appl. Phys.* **47**, 3257 (2008).
- ⁵⁴Y. Nishi, P. A. Maksym, D. G. Austing, T. Hatano, L. P. Kouwenhoven, H. Aoki, and S. Tarucha, *Phys. Rev. B* **74**, 033306 (2006).
- ⁵⁵S. Tarucha and J. Baugh, *J. Phys. Soc. Jpn.* **77**, 031011 (2008).
- ⁵⁶R. Takahashi, K. Kono, S. Tarucha, and K. Ono, *Jpn. J. Appl. Phys.* **49**, 04DJ07 (2010).
- ⁵⁷J. A. McNeil and W. G. Clark, *Phys. Rev. B* **13**, 4705 (1976).
- ⁵⁸J. Lu, M. J. R. Hoch, P. L. Kuhns, W. G. Moulton, Z. Gan, and A. P. Reyes, *Phys. Rev. B* **74**, 125208 (2006).
- ⁵⁹D. J. Reilly, J. M. Taylor, J. R. Petta, C. M. Marcus, M. P. Hanson, and A. C. Gossard, *Phys. Rev. Lett.* **104**, 236802 (2010).